

Low-latency VLSI Architecture for Neural Cross-frequency Coupling Analysis

Gerard O’Leary, *IEEE Student Member*, Taufik A. Valiante and Roman Genov, *IEEE Member*

Abstract— Growing evidence suggests that cross-frequency coupling (CFC) is a key mechanism in neuronal computation, communication, and learning in the brain. Abnormal CFC has been implicated in pathological brain states such as epilepsy and Parkinson’s disease. A reduction in excessive coupling has been shown in effective neuromodulation treatments, suggesting that CFC may be a useful feedback measure in closed-loop neural stimulation devices. However, processing latency limits the responsiveness of such systems. A VLSI architecture is presented which implements three selectable measures of CFC to enable the application specific trade-off between low-latency and high-accuracy processing. The architecture is demonstrated using *in-vitro* human neocortical slice recordings, with a latency of 48ms.

I. INTRODUCTION

Recent studies have found that cross-frequency coupling (CFC) may play a functional role in biological information processing in the brain [1]. In particular, phase-amplitude coupling (PAC) has been hypothesized to provide an effective means to integrate functional systems, transferring information from large-scale brain networks operating at behavioral timescales, to rapid cortical processing [2].

It has been theorized that global brain rhythms modulate the excitability of local neural populations through fluctuations in membrane potentials, increasing the probability of neuronal spiking at a specific phase of slower rhythms [3]. In electroencephalography (EEG), this mechanism manifests itself in local field potentials which resemble amplitude modulation in electronic communication.

Abnormal CFC has been implicated in pathological brain states such as epilepsy and Parkinson’s disease. CFC between pathological high frequency oscillations (pHFOs) and lower frequency rhythms are elevated in the seizure-onset zone compared to non-epileptic regions [4], and exaggerated PAC has been observed in the primary motor cortex of Parkinson’s Disease patients [5]. A reduction in excessive coupling has been shown in effective neuromodulation treatments [6]. This suggests that CFC may be a useful feedback measure for use in closed-loop neural stimulation devices.

G. O’Leary and R. Genov are with The Edward S. Rogers Sr. Department of Electrical & Computer Engineering, University of Toronto, Ontario, Canada, M5S 2E4 ({gerard.oleary, roman}@eecg.utoronto.ca).

T.A. Valiante is with the Division of Neurosurgery, Department of Surgery, University of Toronto, Toronto, Ontario, Canada, M5T 1P5 (e-mail: taufik.valiante@uhn.ca).

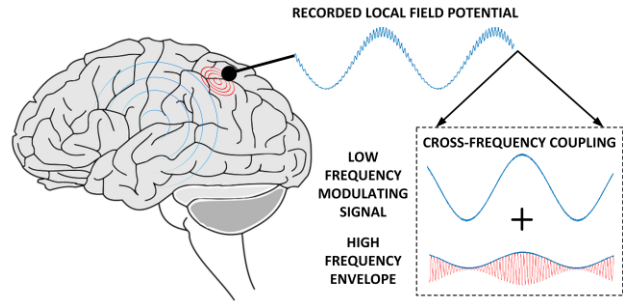


Figure 1. Cross-frequency coupling. Neuronal sub-population activity (red) is modulated by global low-frequency oscillations (blue).

Depending on the application, a tradeoff must be made between precision and computational efficiency. In applications utilizing closed-loop processing based on CFC, a low-latency is required to quickly determine parameters for responsive neural stimulation. Such experiments performed *in-vivo* may require the use of implantable microsystems, which must operate under highly power-constrained conditions. This configurable architecture supports three metrics to enable the application-specific tradeoff between low-power, low-latency and high-precision.

Furthermore, a key computational overhead routinely involves determining the statistical significance of a given measure of CFC. This architecture supports this functionality by efficiently performing surrogate statistical analysis at the expense of increased latency and power-consumption.

II. MEASURING CFC

Three measures of CFC have been implemented to enable an application specific tradeoff between sample latency (τ_s) and precision. The *Cross-Frequency Phase Locking Value* (CF-PLV), has been proposed to detect the cross-frequency synchrony between a low frequency phase and a high frequency envelope phase [7]. The CF-PLV does not quantify the relative amplitude of modulation, and so the *Heights Ratio* (HR) has been implemented to compliment this measurement [2]. The *Mean Vector Length Modulation Index* (MVL-MI) computes the magnitude of an averaged complex-valued time series, where each sample is comprised of the envelope amplitude of a modulated high-frequency signal, and the phase of a low-frequency modulating signal [8]. The VLSI implementation of these methods will be discussed in detail in Section V.

III. SYSTEM ARCHITECTURE

The system architecture is comprised of modulation signal extraction, CFC processing, and surrogate analysis cores as outlined in Figure 2. All processing blocks share common resources, which are time-multiplexed between processing stages. These include a configurable 512-tap Finite Impulse Response (FIR) filter supporting both linear-phase bandpass and Hilbert transform functionality, a dual-core Coordinate Rotation Digital Computer (CORDIC) block which supports both rotational and vectoring modes in a circular configuration, and a 32-bit low-power optimized multiply and accumulate block (MAC).

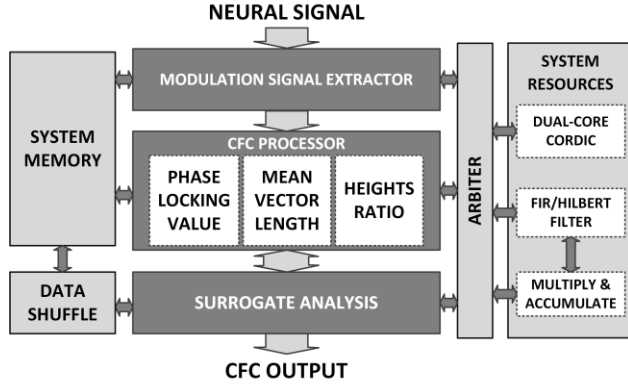


Figure 2. CFC processing system architecture uses shared resources in different configurations to enable the calculation of three selectable metrics.

IV. MODULATION SIGNAL EXTRACTION

The first stage in calculating the implemented cross-frequency metrics involves extracting the “phase-modulating” and “amplitude-modulated” signals. These will be referred to as the phase frequency (f_p) and amplitude frequency envelope (f_A), respectively. Theta modulated high-gamma oscillations have been observed where f_p is in the range 4-8 Hz and the f_A carrier is in the range 50-200 Hz [8].

The raw EEG signal, $x(t)$, is bandpass filtered using a linear-phase FIR filter to extract both $f_p(t)$ and the high-frequency modulated signal. Once the modulated high-gamma component has been isolated, its amplitude envelope time series, $f_A(t)$ can be extracted (Figure 3). An analytic signal is first formed by passing the signal through a Hilbert filter, creating both real and imaginary components. The amplitude of the envelope, $f_A(t)$, can then be extracted by taking the magnitude of the complex vector $f_A(t)$.

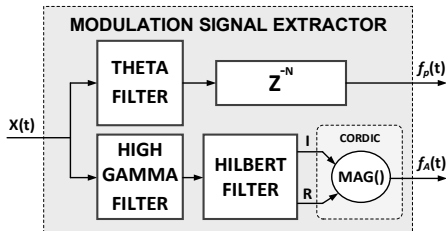


Figure 3. Modulation signal extractor. Extracts high-gamma envelope (f_A) and theta modulating signal (f_p) with filter delay matching.

V. CFC PROCESSOR IMPLEMENTATION

A. Cross-Frequency Phase Locking Value (CF-PLV)

The goal of the CF-PLV algorithm is to detect the cross-frequency synchrony between the phase of the low frequency modulating signal ($\phi_{fp(t)}$), and the phase of the envelope extracted from the high frequency modulated signal ($\phi_{fA(t)}$). The phase difference between both signals is calculated as

$$\Delta\phi(t) = \phi_{fA(t)} - \phi_{fp(t)} \quad (1)$$

This angle is used to create an instantaneous complex vector which is averaged over N samples (2). The magnitude of this average vector is used as a measure of phase locking. If the average $\Delta\phi_i$ is 0, both $f_p(t)$ and $f_A(t)$ are phase-locked.

$$PLV = \frac{1}{N} \sqrt{\left(\sum_{t=0}^{N-1} (\cos(\Delta\phi(t)))\right)^2 + \left(\sum_{t=0}^{N-1} (\sin(\Delta\phi(t)))\right)^2} \quad (2)$$

The VLSI architecture to compute this measure is shown in Figure 4. The envelope time series is first filtered using the same parameters as used for f_p . Following this, analytic signals for both $f_p(t)$ and $f_A(t)$ are created using a Hilbert transform. The PLV is then determined for the phase modulating theta signal and the extracted envelope of the amplitude modulated high-gamma signal.

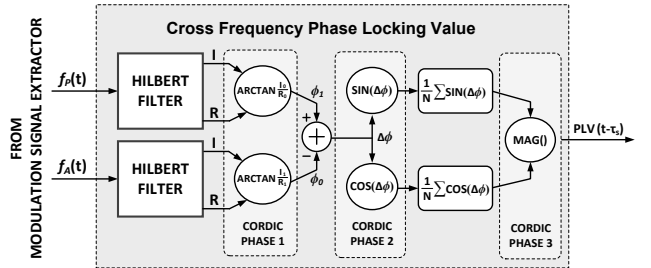


Figure 4. Cross-frequency phase locking value (CF-PLV) architecture.

This implementation of the PLV algorithm offers several advantages over existing solutions [9]. FIR based moving average filters have been replaced by an IIR approximation, resulting in a 60% decrease in latency. Furthermore, the number of CORDIC cores has been reduced from five to two by adding system arbitration to support resource reuse (in Figure 4, only two CORDIC blocks are used at a given time). This optimization results in a silicon area reduction of over 8x with no impact on latency.

B. The Heights Ratio

A limitation of the CF-PLV measure is highlighted in Figure 5, where both 5a and 5b result in the same coupling measure independent of the relative amplitude of modulation.

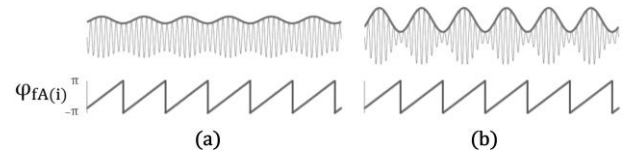


Figure 5. Limitation of CF-PLV. Phase alone does not reflect the intensity of high-frequency modulation, as ϕ_{fA} is the same for (a) and (b).

One method to address this issue involves the use of the Heights Ratio [2] to compliment the CF-PLV value (Figure 6), where h_{max} and h_{min} are the maximum and minimum heights taken from the extracted $f_A(t)$ envelope. When enabled, these values are updated for each new sample.

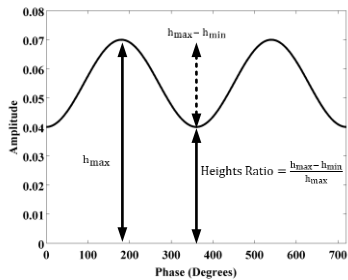


Figure 6. The heights ratio is used to quantify the modulation ratio.

C. Mean Vector Length Modulation Index (MVL-MI)

The mean vector length modulation index (MVL-MI) [8] computes the magnitude of the average value of a complex-valued time series (3). Each sample point is comprised of the amplitude of the modulated high-frequency envelope, and the phase of the low-frequency modulating signal.

$$z(t) = A_{HF} e^{i\phi_{LF}(t)} \quad (3)$$

The time series defined in the complex plane is used to extract a phase-amplitude coupling measure. Each instantaneous amplitude point is represented by the length of the complex vector, whereas the modulating signal phase of the time point is represented by the vector angle. The magnitude of the average complex vector of this time series reflects the raw modulation index.

$$m_{raw} = |\overline{z(t)}| \quad (4)$$

In the case of an absence of phase-amplitude coupling, the plot of the time series in the complex plane is characterized by a roughly uniform circular density of vector points, symmetric around zero (Figure 7).

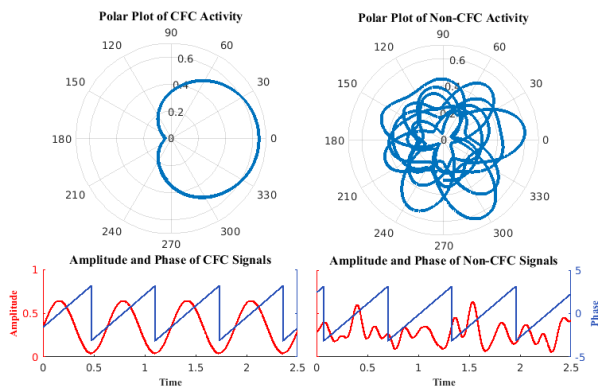


Figure 7. MVL-MI complex vector series. A bump at 0 degrees in the complex plane indicates PAC (Left). A uniform circular density indicates no relationship between phase and amplitude (Right).

If there is modulation of the high-frequency amplitude by the $f_p(t)$ phase, the $f_A(t)$ envelope is higher at certain phases than others. This higher amplitude for certain angles will lead

to a “bump” in the complex plane plot, leading to loss of symmetry around zero. This loss of symmetry can be inferred by measuring the length of the average vector of all points in the complex plane. As a lack of coupling results in a symmetric distribution around zero, the resulting mean vector length is small. The existence of coupling leads to a non-uniform circular distribution, resulting in a larger mean vector length. The MVL-MI is computed as shown in Figure 8 for the phase modulating signal and extracted envelope.

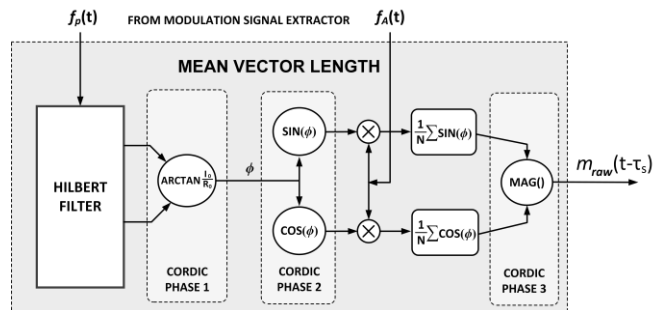


Figure 8. Mean vector length modulation index architecture.

VI. SURROGATE ANALYSIS

To consider the level of statistical significance of the estimated CFC metrics, a surrogate distribution is formed by repeating the computation of either MVL-MI or CF-PLV with shuffled versions of the amplitude signal, $f_A(t)$. This process is accelerated using a random access circular sample buffer which is used for inter-sample memory storage.

The random selection of the start point in each shuffle iteration is performed using a linear feedback shift register (LFSR) as a pseudorandom number generator. This acts as a memory address generator to access a random start points in the circular buffer, from which the surrogate is generated.

The mean, μ , and variance (Mean Absolute Deviation) are calculated across the set of values from each surrogate iteration, which are used to assess the significance of the CFC metric. 50 permutations can be sufficient [7]; however, this can be increased dynamically, depending on the required accuracy.

VII. METHODS

The functionality of the architecture was verified using data obtained at The Toronto Western Hospital [10] under Research Ethic's Board Approval. Local field potentials (LFPs) were recorded simultaneously in superficial (layers II/III) and deep (layers V–VI) layers in 500um thick human temporal cortical slices using a single glass electrode in each layer filled with a solution containing 150 mM NaCl or a standard artificial cerebrospinal fluid (ACSF) (Figure 9).

Signals were acquired at 10 kHz (low pass at 5 kHz). Recordings were obtained at 36°C in standard ACSF perfusion (baseline), during kainate (50 nM) applications, and during kainate plus carbachol (50 M) conditions.

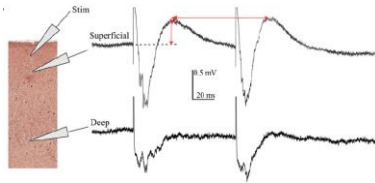


Figure 9. Slice electrode arrangement for signal acquisition [10].

For each slice, a single 30 s region displaying the largest power increase during kainate plus carbachol conditions was analyzed. A sub segment of PAC detected in [6] was used to demonstrate the functionality of the architecture (Figure 10), and was downsampled to a 1kHz sample rate.

VIII. RESULTS

The accuracy of each metric is evaluated using 16-bit fixed point implementation (Figure 10). Both CF-PLV and the MVL-MI are sensitive to the intensity of PAC. CF-PLV has a range of 0 to 1 and MVL-MI is unconstrained.

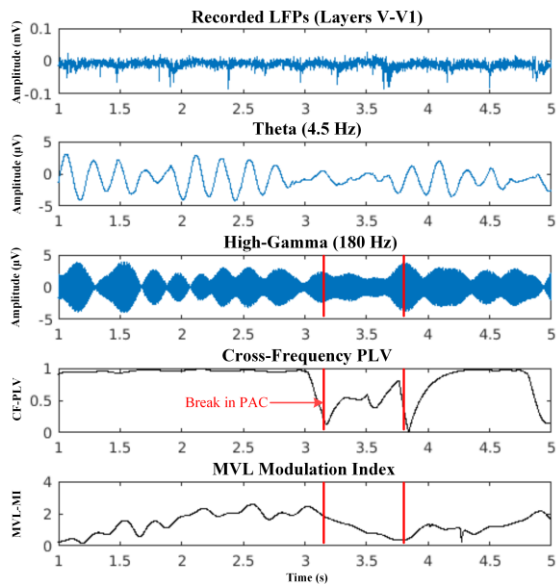


Figure 10. Computed measures of PAC using MVL-MI and CF-PLV.

The output latency for each reported metric is shown in Figure 11. HR offers the lowest processing latency with a sample latency equivalent to that of MVL-MI. While the introduction of surrogate analysis does not impact the sample latency, the processing latency increases almost linearly with each iteration as the metric is computed for each surrogate. A greater number of CPU cycles directly increases the power required for a given CFC metric.

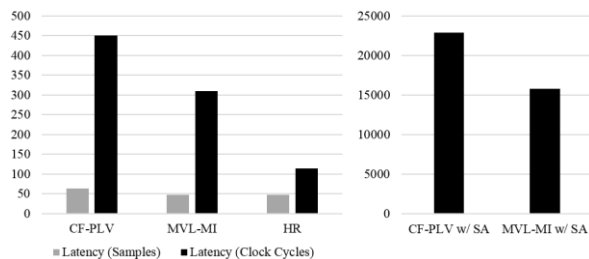


Figure 11. Processing and sample latency comparison (Left). And the overhead to perform surrogate analysis ($n=50$) for a metric (Right).

IX. CONCLUSION

In this paper, a VLSI architecture is presented to detect cross-frequency coupling in neural signals and is validated using in-vitro human slice recordings. The processing latency has been minimized to enable highly-responsive interaction with neural systems under investigation.

For better time resolution and precision, CF-PLV has been demonstrated. However, this measurement comes at the expense of increased latency. The MVL-MI offers a good tradeoff between power and latency, but relies more heavily on surrogate analysis for de-biasing [8]. The Heights Ratio comes at the lowest computational expense, but is sensitive to noise and certain amplitude distributions [2]. This architecture implements these measures with a power efficiency suitable for implantable devices, enabling responsive closed-loop *in-vivo* experiments involving CFC.

REFERENCES.

- [1] B. Voloh, T. et al., "Theta-gamma coordination between anterior cingulate and prefrontal cortex indexes correct attention shifts," Proceedings of the National Academy of Sciences, vol. 112, no. 27, pp. 8457–8462, Jul. 2015.
- [2] A. B. L. Tort et al., "Measuring Phase-Amplitude Coupling Between Neuronal Oscillations of Different Frequencies," Journal of Neurophysiology, vol. 104, no. 2, pp. 1195–1210, Aug. 2010.
- [3] R. T. Canolty and R. T. Knight, "The functional role of cross-frequency coupling," Trends in Cognitive Sciences, vol. 14, no. 11, pp. 506–515, Nov. 2010.
- [4] M. Guirgis et al., "The role of delta-modulated high frequency oscillations in seizure state classification," in 2013 35th Annual International Conference of the IEEE Engineering in Medicine and Biology Society (EMBC), 2013, pp. 6595–6598.
- [5] De Hemptinne, Coralie et al. "Exaggerated Phase-amplitude Coupling in the Primary Motor Cortex in Parkinson Disease." Proceedings of the National Academy of Sciences of the United States of America 110.12 (2013): 4780–4785, 28 Apr. 2017.
- [6] C. de Hemptinne et al., "Therapeutic deep brain stimulation reduces cortical phase-amplitude coupling in Parkinson's disease," Nature Neuroscience, vol. 18, no. 5, pp. 779–786, Apr. 2015.
- [7] W. D. Penny et al., "Testing for nested oscillation," Journal of Neuroscience Methods, vol. 174, no. 1, pp. 50–61, Sep. 2008.
- [8] R. T. Canolty et al., "High Gamma Power Is Phase-Locked to Theta Oscillations in Human Neocortex," Science, vol. 313, no. 5793, pp. 1626–1628, Sep. 2006.
- [9] K. Abdelhalim et al., "VLSI multivariate phase synchronization epileptic seizure detector," in Neural Engineering (NER), 2011 5th International IEEE/EMBS Conference on, 2011, pp. 461–464.
- [10] C. M. Florez et al., "In Vitro Recordings of Human Neocortical Oscillations," Cerebral Cortex, vol. 25, no. 3, pp. 578–597, Mar. 2015.